

Cluster Gauss-Newton method for sampling multiple solutions of nonlinear least squares problems - with applications to pharmacokinetic models

Yasunori Aoki* Ken Hayami† Kota Toshimoto‡ Yuichi Sugiyama§

October 26, 2021

Abstract

Parameter estimation problems of mathematical models can often be formulated as nonlinear least squares problems. Typically these problems are solved numerically using iterative methods. The solution obtained using these iterative methods usually depends on the choice of the initial iterate. Especially, when there is no unique minimum to the nonlinear least squares problem, the algorithm finds one of the solutions near the initial iterate. Hence, the estimated parameter and subsequent analyses using the estimated parameter depends on the choice of the initial iterate. One way to reduce the analysis bias due to the choice of the initial iterate is to repeat the algorithm from multiple initial iterates. However, the procedure can be computationally intensive and is not often implemented in practice. To overcome this problem, we propose the Cluster Gauss-Newton (CGN) method, an efficient algorithm for finding multiple possible solutions of nonlinear-least squares problems. The algorithm simultaneously solves the nonlinear least squares problem from multiple initial iterates. The algorithm iteratively improves the solutions from these initial iterates similarly to the Gauss-Newton method. However, it uses a global linear approximation instead of the gradient. The global linear approximations are computed collectively among all the initial iterates to minimise the computational cost and increase the robustness against convergence to local minima. We use mathematical models used in pharmaceutical drug development to demonstrate its use and that the proposed algorithm is computationally more efficient and more robust against local minima compared to the Levenberg-Marquardt method.

1 Introduction

The parameter estimation of mathematical models often boils down to solving nonlinear least squares problems. Hence, algorithms for solving nonlinear least squares problems are widely used in many scientific fields. Most of the algorithms for solving nonlinear least squares problems focus on finding a single solution. On the other hand, there is very limited methodological development on algorithms for finding multiple solutions of nonlinear least squares problems when the solution is not unique. Standard methods such as the Levenberg-Marquardt method can find a solution of a nonlinear least squares problem that does not have a unique solution. However, the parameter found by the algorithm depends on the choice of the initial

*Visiting Associate Professor, National Institute of Informatics, 2-1-2 Hitotsubashi, Chiyoda, Tokyo 101-8430, Japan, and Visiting Researcher, Sugiyama Laboratory, RIKEN Baton Zone Program, 1-7-22 Suehiro-cho, Tsurumi-ku, Yokohama, Kanagawa 230-0045, Japan (yaoki@uwaterloo.ca).

†National Institute of Informatics, and SOKENDAI (The Graduate University for Advanced Studies), 2-1-2 Hitotsubashi, Chiyoda, Tokyo 101-8430, Japan (hayami@nii.ac.jp). The author was supported in part by JSPS KAKENHI Grant Number 15K04768 and 15H02968.

‡Sugiyama Laboratory, RIKEN Baton Zone Program, 1-7-22 Suehiro-cho, Tsurumi-ku, Yokohama, Kanagawa 230-0045, Japan.

§Sugiyama Laboratory, RIKEN Baton Zone Program, 1-7-22 Suehiro-cho, Tsurumi-ku, Yokohama, Kanagawa 230-0045, Japan.

iterate. To reduce the analysis bias due to the initial iterate used for the algorithm, it is a good practice to repeatedly use the algorithm with various initial iterates to gain the understanding of the influence of the initial iterates. On the other hand, due to the computational challenges and cost, it is rarely done in practice. In this paper, we propose a new computational method for efficiently finding multiple solutions to nonlinear least squares problems.

Our algorithm development for finding multiple solutions of nonlinear least squares problems was motivated by a mathematical model of pharmaceutical drug concentration in a human body called the physiologically based pharmacokinetic (PBPK) model. The PBPK model is typically a system of mildly nonlinear stiff ordinary differential equations (ODEs) with many parameters. This type of mathematical model is constructed based on the knowledge of the mechanism of how the drug is absorbed, distributed, metabolised and excreted. Given the complexity of this process and the limitation of the observations we can obtain from a live human subject, the model parameters cannot be uniquely identified from the observations. The estimated parameters of the PBPK model are used to simulate the drug concentration of the patient from whom we are often unable to test the drug on (e.g., children, pregnant person, a person with rare genetic anomaly) or to predict the experiment that is yet to be run (different amount of drug administration, multiple drug used at the same time). As the simulated drug concentration is used to predict the safety of the drug in these different scenarios, it is essential to consider the multiple predictions based on multiple possible parameters that are estimated from the available observation. A motivating example is presented in Appendix A.

In [1, 2] we proposed the Cluster Newton (CN) method, which is a computationally efficient method for obtaining multiple solutions of **a system of nonlinear equations**. In recent years CN has been used in the field of pharmaceutical science [19, 6, 3, 15, 10, 11] and shown to be useful for the applications. For example, [15] used the parameters estimated by CN to predict the drug adverse effect, [11] used the estimated parameters to predict the outcome of a clinical trial. However, based on these applications of CN, we observed the necessity for an algorithm to find multiple solutions of **a nonlinear least squares problem**. (See Appendix B.)

1.1 Nonlinear least squares problem of our interest

In this paper, we propose an algorithm for obtaining multiple solutions of a nonlinear least squares problem

$$\min \|\mathbf{f}(\mathbf{x}) - \mathbf{y}^*\|_2 \quad (1)$$

that does not have a unique solution, that is to say, there exist $\mathbf{x}^{(1)} \neq \mathbf{x}^{(2)}$ such that

$$\min \|\mathbf{f}(\mathbf{x}) - \mathbf{y}^*\|_2 = \|\mathbf{f}(\mathbf{x}^{(1)}) - \mathbf{y}^*\|_2 = \|\mathbf{f}(\mathbf{x}^{(2)}) - \mathbf{y}^*\|_2. \quad (2)$$

Here, \mathbf{f} is a nonlinear function from \mathbb{R}^n to \mathbb{R}^m , $\mathbf{x}^{(1)}, \mathbf{x}^{(2)} \in \mathbb{R}^n$ and $\mathbf{y}^* \in \mathbb{R}^m$. The nonlinear function \mathbf{f} can be derived from a mathematical model, the vector \mathbf{x} can be regarded as a set of model parameters which one wishes to estimate, and the vector \mathbf{y}^* can be regarded as a set of observations one wishes to fit the model to.

In order to make our algorithm as generally applicable as possible and to make it easier to use for a wide variety of applications, we assume the nonlinear function \mathbf{f} to be a "black-box". More specifically, we assume the case where derivatives of \mathbf{f} with respect to \mathbf{x} are not readily available or the case where \mathbf{f} is not differentiable.

We shall call the following quantity the sum of squares residual (SSR):

$$\|\mathbf{f}(\mathbf{x}) - \mathbf{y}^*\|_2^2, \quad (3)$$

and use it for the quantification of the goodness of \mathbf{x} as the approximation of the solution of the least squares problem (1).

1.2 A toy example

To illustrate a least squares problem without a unique solution, we present the following simple toy example. Let there be an experiment where the observations can be written as a random variable below:

$$u^*(t) = t + \epsilon, \tag{4}$$

where ϵ is a random variable drawn from the normal distribution of mean 0 standard deviation 0.1 (i.e., $\epsilon \sim \mathcal{N}(0,0.1)$), and t is the time of the observation. Let us consider the case where we sample five times e.g., $t_1 = 1, t_2 = 2, t_3 = 3, t_4 = 4, t_5 = 5$ and denote these observations as a vector $\mathbf{y}^* = [u^*(1), u^*(2), u^*(3), u^*(4), u^*(5)]^T$.

We now consider a case where one has constructed a mathematical model to model this observation as follows:

$$u(t; \theta_1, \theta_2) = \frac{\theta_1}{\theta_2}t, \tag{5}$$

where θ_1 and θ_2 are model parameters. We can now write the parameter estimation problem from the observation data \mathbf{y}^* as the following least squares problem

$$\min \|\mathbf{f}(\mathbf{x}) - \mathbf{y}^*\|_2 \tag{6}$$

where $\mathbf{x} = [\theta_1, \theta_2]^T$ and

$$\mathbf{f}(\mathbf{x}) = [u(1; \theta_1, \theta_2), u(2; \theta_1, \theta_2), u(3; \theta_1, \theta_2), u(4; \theta_1, \theta_2), u(5; \theta_1, \theta_2)]^T. \tag{7}$$

As can be seen trivially from equation (5), this is an over parameterised model and the least squares problem (6) has infinitely many solutions with $\alpha = \frac{\theta_1}{\theta_2}$ where α is a constant close to 1.

For this toy model, deriving the relationship $\alpha = \frac{\theta_1}{\theta_2}$ is trivial. Hence, we can analytically reparameterise the model. However, for a more complex model structure, such a relationship may not be easily expressed analytically.

2 Method: Algorithm

In this section we describe the proposed algorithm. We first introduce a rough concept using a toy example in Subsection 2.1 and then introduce the full algorithm in detail in Subsectin 2.2.

2.1 Brief explanation of the algorithm

The aim of the proposed Cluster Gauss-Newton (CGN) algorithm is to efficiently find multiple solutions of the nonlinear least squares problem (1). We do so by first creating a collection of initial guesses which we call the ‘cluster’. Then, we move the cluster iteratively using a linear approximation of the nonlinear function \mathbf{f} , similarly to the Gauss-Newton method [4].

The unique idea in our CGN method is that the linear approximation is constructed collectively throughout the points in the cluster instead of using the Jacobian matrix which approximates the nonlinear function linearly at a point. By using points in the cluster to construct the linear approximation, we avoid extra computation of the nonlinear function for approximating the Jacobian matrix. This idea of approximating the nonlinear function collectively using the points in the cluster was utilised in CN [2]. In the proposed method, we further improve on the way we do the linear approximation.

In order to visualise the key differences between these linear approximations, we consider the nonlinear function $f = x^2 - 2\cos(10x)$ and aim to find x that minimises this nonlinear function (cf. Figure 1). The global minimum of this function is -2 at $x = 0$. The randomly generated points in the initial cluster is located at:

$$\begin{aligned} x_1 &= -3.3797853, & x_2 &= -1.1656025, & x_3 &= -0.6145728, \\ x_4 &= 1.1540421, & x_5 &= 2.0755468, \end{aligned} \tag{8}$$

as indicated by the red dots. We now compute the linear approximations used to move these points in the cluster to minimise the function f .

Gradient

For this nonlinear function, the gradient at x_i is $f'(x_i) = 2x_i + 20\sin(10x_i)$. Practically, when f is a “black box”, we can approximate the gradient by a finite difference scheme, for example, $f'(x_i) \approx \frac{f(x_i+\epsilon) - f(x_i)}{\epsilon}$. Then, the linear approximation at x_i can be written as $f(x) \approx \frac{f(x_i+\epsilon) - f(x_i)}{\epsilon}(x - x_i) + f(x_i)$. Notice that it requires one extra evaluation of f at $x_i + \epsilon$ for each x_i . This number of extra function evaluation is, in general, proportional to the dimension of the independent variable of the nonlinear function.

Cluster Newton (CN) method

In CN, we construct one linear approximation for all points in the cluster in the following way.

$$\min_{a,b} \sum_{i=1}^5 |ax_i + b - f(x_i)|_2^2 \tag{9}$$

where a is the slope and b is the intercept of the linear approximation, i.e., $f(x) = ax + b$. Note that for CN, we have designed to construct the cluster with more number of points in the cluster than the dimension of the independent variable of the nonlinear function. Thus equation(9) can be regarded as a least squares solution of an over determined system of linear equations. Note that we do not need any extra evaluations of f in order to determine the linear approximation.

Cluster Gauss-Newton (CGN) method (proposed method)

In the proposed method, we construct a linear approximation for each point in the cluster while using the other points in the cluster to globally approximate the nonlinear function with the linear function. The influence of another point in the cluster to the linear approximation is weighted according to how close the point is to the point of approximation, i.e.,

$$\min_{a^{(i)}} \sum_{i \neq j} \left| \frac{a^{(i)}(x_j - x_i) + f(x_i) - f(x_j)}{(x_j - x_i)^{2\gamma}} \right|^2 \tag{10}$$

where $a^{(i)}$ is the slope of the linear approximation at x_i and the linear approximation at x_i can be written as $f(x) = a^{(i)}(x - x_i) + f(x_i)$, and $\gamma \geq 0$ is a constant. Note that Equation(10) can also be regarded as a weighted least squares solution of an overdetermined system of linear equations. The weight is motivated by the fact that we weight the information from the neighbouring points in the cluster more than the ones further away when constructing the linear approximation. Again, note that we do not require any extra evaluation of f for obtaining these linear approximations.

We have depicted the linear approximations at each point in the initial cluster in Figure 1. As can be seen, the regular gradient captures the local behaviour of the nonlinear function. Hence, it is bound to converges to a local minimum. CN captures the global behaviour of the nonlinear function. Hence, 3 out of 5 points move towards the global minimum following the linear approximation. However, as we are approximating the nonlinear function at all points with one linear function, it is not appropriate for some points. The proposed CGN method, does on the other hand, capture both the global behaviour of the nonlinear function while having one linear approximation each for each point. Thus, in this example, all points will descend to the global minimum if the points are moved based on the slope of the linear approximations.

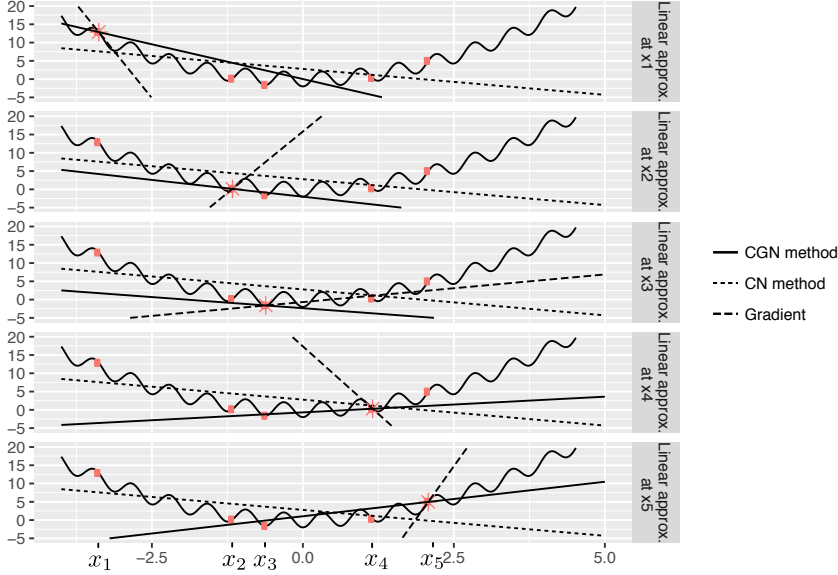


Figure 1: Schematic comparison of the linear approximations.

2.2 Detailed description of the algorithm

Next, we describe the new algorithm in detail. In this subsection describing the algorithm, we denote a scalar quantity with a lower case letter (e.g., a , c), a matrix with a capital letter, for example A , or M , and a column vector by a bold symbol of a lower case letter, (e.g., \mathbf{v} , \mathbf{a}), unless otherwise specifically stated. Super script T indicates the transpose. Hence, \mathbf{v}^T and \mathbf{a}^T are row vectors.

1) Pre-iteration process

The initial iterate of CGN, a set of vectors $\{\mathbf{x}_i^{(0)}\}_{i=1}^N$ are randomly generated following a uniform distribution within the lower bound \mathbf{x}^L and upper bound \mathbf{x}^U given by the user as the initial estimate of the plausible location of the solution. That is to say, the value $x_{ji}^{(0)}$ is a sample from $\mathcal{U}(x_j^L, x_j^U)$, where $x_{ji}^{(0)}$ is the j th element of vector $\mathbf{x}_i^{(0)}$.

Store the initial set of vectors in a matrix $X^{(0)}$, i.e.,

$$X^{(0)} = [\mathbf{x}_1^{(0)}, \mathbf{x}_2^{(0)}, \dots, \mathbf{x}_N^{(0)}] \quad (11)$$

where the super script (0) indicates the initial iterate.

Evaluate the nonlinear function \mathbf{f} at each \mathbf{x}_i and store in matrix $Y^{(0)}$, i.e.,

$$Y^{(0)} = [\mathbf{f}(\mathbf{x}_1^{(0)}), \mathbf{f}(\mathbf{x}_2^{(0)}), \dots, \mathbf{f}(\mathbf{x}_N^{(0)})]. \quad (12)$$

If the function \mathbf{f} cannot be evaluated at $\mathbf{x}_i^{(0)}$, then re-sample $\mathbf{x}_i^{(0)}$ until \mathbf{f} can be evaluated. Compute the sum of squares residual vector $\mathbf{r}^{(0)}$, i.e.,

$$\mathbf{r}^{(0)} = \left[\|\mathbf{f}(\mathbf{x}_1^{(0)}) - \mathbf{y}^*\|_2^2, \|\mathbf{f}(\mathbf{x}_2^{(0)}) - \mathbf{y}^*\|_2^2, \dots, \|\mathbf{f}(\mathbf{x}_N^{(0)}) - \mathbf{y}^*\|_2^2 \right]^T. \quad (13)$$

Fill the regularisation parameter vector $\boldsymbol{\lambda}^{(0)} \in \mathbb{R}^N$, with the user-specified initial regularisation parameter λ_{init} .i.e.,

$$\boldsymbol{\lambda}^{(0)} = [\lambda_{\text{init}}, \lambda_{\text{init}}, \dots, \lambda_{\text{init}}]^T. \quad (14)$$

2) Main iteration

Repeat the following procedure until the user specified stopping criteria are met. We denote the iteration number as k , which starts with 0 and is incremented by 1 after each iteration.

2-1) Construct weighted linear approximations of the nonlinear function

We first construct a linear approximation around the point $\mathbf{x}_i^{(k)}$, i.e.,

$$\mathbf{f}(\mathbf{x}) \approx A_{(i)}^{(k)}(\mathbf{x} - \mathbf{x}_i^{(k)}) + \mathbf{f}(\mathbf{x}_i^{(k)}). \quad (15)$$

Here, $A_{(i)}^{(k)} \in \mathbb{R}^{m \times n}$ describes the ‘‘global slope’’ of the linear approximation around $\mathbf{x}_i^{(k)}$.

The key difference of our algorithm compared to others is that we approximate the Jacobian like matrix $A_{(i)}^{(k)}$ collectively using all the function evaluations of \mathbf{f} in the previous iteration, i.e.,

$$\begin{aligned} A_{(i)}^{(k)} &= \operatorname{argmin}_{A \in \mathbb{R}^{m \times n}} \sum_{j=1}^N \left[d_{j(i)}^{(k)} \left\| \mathbf{f}(\mathbf{x}_j^{(k)}) - \left\{ A \left(\mathbf{x}_j^{(k)} - \mathbf{x}_i^{(k)} \right) + \mathbf{f}(\mathbf{x}_i^{(k)}) \right\} \right\|_2 \right]^2 \\ &= \operatorname{argmin}_{A \in \mathbb{R}^{m \times n}} \sum_{j=1}^N \left(d_{j(i)}^{(k)} \left\| \Delta \mathbf{y}_{j(i)}^{(k)} - A \Delta \mathbf{x}_{j(i)}^{(k)} \right\|_2 \right)^2 \end{aligned} \quad (16)$$

for $i = 1, \dots, N$, where $d_{j(i)}^{(k)} \geq 0$, $j = 1, \dots, N$ are weights. Here, $\Delta \mathbf{y}_{j(i)}^{(k)} = \mathbf{f}(\mathbf{x}_j^{(k)}) - \mathbf{f}(\mathbf{x}_i^{(k)}) \in \mathbb{R}^m$ and $\Delta \mathbf{x}_{j(i)}^{(k)} = \mathbf{x}_j^{(k)} - \mathbf{x}_i^{(k)} \in \mathbb{R}^n$. (Note that $\Delta \mathbf{y}_{i(i)}^{(k)} = \mathbf{0}$, $\Delta \mathbf{x}_{i(i)}^{(k)} = \mathbf{0}$.)

Also, let

$$\Delta Y_{(i)}^{(k)} = \left[\Delta \mathbf{y}_{1(i)}^{(k)}, \Delta \mathbf{y}_{2(i)}^{(k)}, \dots, \Delta \mathbf{y}_{N(i)}^{(k)} \right] \in \mathbb{R}^{m \times N} \quad (17)$$

$$\Delta X_{(i)}^{(k)} = \left[\Delta \mathbf{x}_{1(i)}^{(k)}, \Delta \mathbf{x}_{2(i)}^{(k)}, \dots, \Delta \mathbf{x}_{N(i)}^{(k)} \right] \in \mathbb{R}^{n \times N}. \quad (18)$$

Note that $\mathbf{f}(\mathbf{x}_i^{(k)})$ are always computed at the previous iteration (e.g., as equation (12) when $k = 0$ and in Step 2-3 when $k > 0$). Hence, no new evaluation of \mathbf{f} is required at this step.

The key idea here is that we weight the information of the function evaluation near $\mathbf{x}_i^{(k)}$ more than the function evaluation further away. That is to say, $d_{j(i)}^{(k)} > d_{j'(i)}^{(k)}$ if $\|\mathbf{x}_j^{(k)} - \mathbf{x}_i^{(k)}\| < \|\mathbf{x}_{j'}^{(k)} - \mathbf{x}_i^{(k)}\|$.

More specifically, we obtain matrix $A_{(i)}^{(k)}$ row by row by solving the following linear least squares problem using the CGNR (CGLS) algorithm [4, 13] setting the initial iterate as $\boldsymbol{\alpha} = \mathbf{0}$. Here, methods based on the QR decomposition could also be used [4]. However, using the CGNR has the advantage that it does not break down even though $\Delta X_{(i)}^{(k)T}$ is rank-deficient[9].

$$\boldsymbol{\alpha}_{j(i)}^{(k)} = \operatorname{argmin}_{\boldsymbol{\alpha} \in \mathbb{R}^n} \left\| D_{(i)}^{(k)} \left(\Delta X_{(i)}^{(k)T} \boldsymbol{\alpha} - \Delta \boldsymbol{\eta}_{j(i)}^{(k)} \right) \right\|_2 \quad (19)$$

for $i = 1, \dots, N$ and $j = 1, \dots, m$, where $\boldsymbol{\alpha}_{j(i)}^{(k)T}$ is the j th row of matrix $A_{(i)}^{(k)}$,

$$D_{(i)}^{(k)} = \operatorname{diag} \left(d_{1(i)}^{(k)}, d_{2(i)}^{(k)}, \dots, d_{N(i)}^{(k)} \right), \quad (20)$$

and $\boldsymbol{\eta}_{j(i)}^{(k)} \in \mathbb{R}^n$ is the j th column vector of matrix $\Delta Y_{(i)}^{(k)T}$, i.e.,

$$\Delta Y_{(i)}^{(k)T} = \left[\Delta \boldsymbol{\eta}_{1(i)}^{(k)}, \Delta \boldsymbol{\eta}_{2(i)}^{(k)}, \dots, \Delta \boldsymbol{\eta}_{m(i)}^{(k)} \right] \in \mathbb{R}^{N \times m}. \quad (21)$$

See Appendix C for the derivation of equation (19).

For our numerical experiments, we have chosen the weights as

$$d_{j(i)}^{(k)} = \begin{cases} \left(\frac{1}{\sum_{l=1}^n ((x_{lj}^{(k)} - x_{li}^{(k)}) / (x_l^U - x_l^L))^2} \right)^\gamma & \text{if } j \neq i \\ 0 & \text{if } j = i \end{cases}, \quad (22)$$

where $x_{lj}^{(k)}$, x_l^U , x_l^L are the l th element of the vectors $\mathbf{x}_j^{(k)}$, \mathbf{x}^U , \mathbf{x}^L , respectively ($l = 1, \dots, n$), and $\gamma \geq 0$ is a constant. The distance between \mathbf{x}_i and \mathbf{x}_j are normalised by the upper and lower bounds of the initial iterate (i.e., \mathbf{x}^U and \mathbf{x}^L). The effect of the weight $d_{j(i)}^{(k)}$ is analysed in Appendix D.

2-2) Solve for \mathbf{x} that minimizes $\|\mathbf{y}^* - (A_{(i)}^{(k)}(\mathbf{x} - \mathbf{x}_i^{(k)}) + \mathbf{f}(\mathbf{x}_i^{(k)}))\|_2^2$

We now approximate $X^{(k+1)}$ using the matrices $\{A_{(i)}^{(k)}\}_{i=1}^N$ similarly to the Gauss-Newton method with Tikhonov regularisation (e.g., [8, 4]), i.e.,

$$\mathbf{x}_i^{(k+1)} = \mathbf{x}_i^{(k)} + \left(A_{(i)}^{(k)\top} A_{(i)}^{(k)} + \lambda_i^{(k)} I \right)^{-1} A_{(i)}^{(k)\top} (\mathbf{y}^* - \mathbf{y}_i^{(k)}) \quad (23)$$

for $i = 1, \dots, N$,

where \mathbf{y}^* is the set of observations one wishes to fit the nonlinear function \mathbf{f} to (cf. (1)), and $\mathbf{y}_i^{(k)} \equiv \mathbf{f}(\mathbf{x}_i^{(k)})$. Here also, we use CGNR to avoid breakdown when $A_{(i)}^{(k)}$ is rank-deficient. The importance of the regularisation can be seen in the numerical experiment presented in Appendix E.

2-3) Update matrices X and Y and vectors \mathbf{r} and λ

Evaluate the nonlinear function \mathbf{f} for each $\mathbf{x}_i^{(k+1)}$ and store in matrix $Y^{(k+1)}$ similarly to equation (12), calculate the residual vector $\mathbf{r}^{(k+1)}$ similarly to equation (13).

We now revert to $\mathbf{x}_i^{(k)}$ and increment the regularisation parameter if the residual does not decrease, i.e.,

if $r_i^{(k)} < r_i^{(k+1)}$ or $\mathbf{f}(\mathbf{x}_i^{(k+1)})$ can not be evaluated, then let

$$\mathbf{x}_i^{(k+1)} = \mathbf{x}_i^{(k)} \quad (24)$$

$$\mathbf{y}_i^{(k+1)} = \mathbf{y}_i^{(k)} \quad (25)$$

$$\lambda_i^{(k+1)} = 10 \lambda_i^{(k)} \quad (26)$$

else decrease the regularisation parameter, i.e.,

$$\lambda_i^{(k+1)} = \frac{1}{10} \lambda_i^{(k)}, \quad (27)$$

for each $i = 1, \dots, N$.

3 Numerical Experiment

To illustrate the advantages of the proposed algorithm, we have conducted numerical experiments.

3.1 Numerical Experiment setup

In this section we specify the detail of thje numerical experiments.

3.1.1 Mathematical models

For this numerical experiment, we have used the following three published mathematical models of drug concentration in the blood of a human body (PBPK model). The time course drug concentration was simulated from the model, and random noise was added to mimic the observation uncertainties. The simulated drug concentration was used as the observation, and multiple possible parameters were estimated using CGN and conventional nonlinear least squares solvers.

Example 1: Multi-dose problem

For this example, we consider the case where three different amounts of the drug is given (low-dose, medium-dose, and high-dose) orally as pills to a patient. This can be modelled using the same mathematical model as in the Motivating Example (cf. Appendix A, F, and G). The initial value problem of this mathematical model can be written as:

$$\frac{d\mathbf{u}}{dt} = \mathbf{g}(\mathbf{u}, t; \mathbf{x}), \quad (28)$$

$$u_i(t=0) = 0 \quad \text{for } i = 1, \dots, 17, 19, 20, \quad (29)$$

$$u_{18}(t=0) = \begin{cases} 30000 & \text{for low-dose,} \\ 100000 & \text{for medium-dose,} \\ 300000 & \text{for high-dose.} \end{cases} \quad (30)$$

In this mathematical model, $u_1(t)$ represents the drug concentration in blood at time t . For convenience, we denote the drug concentration at time t when the low-dose, medium-dose, and high-dose are given as $u_1^l(t; \mathbf{x})$, $u_1^m(t; \mathbf{x})$, and $u_1^h(t; \mathbf{x})$, respectively. Note that the right hand side of the system of ODEs (28) depends on the parameter vector \mathbf{x} . Hence, the solution of the system of ODEs \mathbf{u} depends not only on t but also on \mathbf{x} . For this example, we consider the case where the blood sample is taken at $t = 2, 3, 4, 6, 8, 12, 24, 36, 48, 72$, so that the nonlinear function \mathbf{f} in (1) can be written as

$$\begin{aligned} \mathbf{f}(\mathbf{x}) = & [u_1^l(2; \mathbf{x}), u_1^l(3; \mathbf{x}), u_1^l(4; \mathbf{x}), u_1^l(6; \mathbf{x}), u_1^l(8; \mathbf{x}), u_1^l(12; \mathbf{x}), u_1^l(24; \mathbf{x}), u_1^l(36; \mathbf{x}), \\ & u_1^l(48; \mathbf{x}), u_1^l(72; \mathbf{x}), u_1^m(2; \mathbf{x}), u_1^m(3; \mathbf{x}), u_1^m(4; \mathbf{x}), u_1^m(6; \mathbf{x}), u_1^m(8; \mathbf{x}), u_1^m(12; \mathbf{x}), \\ & u_1^m(24; \mathbf{x}), u_1^m(36; \mathbf{x}), u_1^m(48; \mathbf{x}), u_1^m(72; \mathbf{x}), u_1^h(2; \mathbf{x}), u_1^h(3; \mathbf{x}), u_1^h(4; \mathbf{x}), u_1^h(6; \mathbf{x}), \\ & u_1^h(8; \mathbf{x}), u_1^h(12; \mathbf{x}), u_1^h(24; \mathbf{x}), u_1^h(36; \mathbf{x}), u_1^h(48; \mathbf{x}), u_1^h(72; \mathbf{x})]^T. \end{aligned}$$

This example is based on [6].

Example 2: intravenous injection and oral administration problem

For this example, we consider the case where the drug is administered via injection into the vein (i.v.) and the case where the drug is given orally as a pill (p.o.) to a patient. This was modelled using a mathematical model similar to the Motivating Example. The initial value problem of this mathematical model for i.v. administration can be written as:

$$\frac{d\mathbf{u}}{dt} = \tilde{\mathbf{g}}(\mathbf{u}, t; \mathbf{x}), \quad (31)$$

$$u_1(t=0) = \frac{30.488}{0.074 + 10^{x_4}}, \quad (32)$$

$$u_i(t=0) = 0 \quad \text{for } i = 2, 3, \dots, 20, \quad (33)$$

where x_4 is one of the parameters in the parameter vector \mathbf{x} . The initial value problem of this mathematical model for p.o. administration can be written as:

$$\frac{d\mathbf{u}}{dt} = \tilde{\mathbf{g}}(\mathbf{u}, t; \mathbf{x}), \quad (34)$$

$$u_i(t=0) = 0 \quad \text{for } i = 1, \dots, 20, \quad (35)$$

$$u_{18} \left(t = \frac{e^{x_{11}}}{2(1 + e^{x_{11}})} \right) = 30.488, \quad (36)$$

$$u_i \left(t = \frac{e^{x_{11}}}{2(1 + e^{x_{11}})} \right) = 0 \quad \text{for } i = 1, \dots, 17, 19, 20, \quad (37)$$

where x_{11} is one of the parameters in the parameter vector \mathbf{x} . $\frac{e^{x_{11}}}{2(1+e^{x_{11}})}$ is the delay in the absorption of the drug (for example the time it takes from intake in the mouth to pill being dissolved in the stomach). Similarly to Example 1, the observable quantity, the drug concentration in blood plasma is represented as $u_1(t; \mathbf{x})$. For convenience, we denote the drug concentration at time t when the drug is administrated by i.v. and p.o. administrations as $u_1^i(t; \mathbf{x})$ and $u_1^p(t; \mathbf{x})$, respectively. For this example, we consider the case where the blood sample is taken at $t = 0.0833, 0.1667, 0.25, 0.5, 0.75, 1, 1.5, 2, 3, 4, 6, 8$ when the drug is given as intravenous injection and the blood sample is taken at $t = 0.5, 1, 1.5, 2, 3, 4, 6, 8, 12, 14$ when the drug is given as a pill orally. The nonlinear function \mathbf{f} can be written as

$$\begin{aligned} \mathbf{f}(\mathbf{x}) = & [u_1^i(0.0833; \mathbf{x}), u_1^i(0.1667; \mathbf{x}), u_1^i(0.25; \mathbf{x}), u_1^i(0.5; \mathbf{x}), u_1^i(0.75; \mathbf{x}), u_1^i(1; \mathbf{x}), \\ & u_1^i(1.5; \mathbf{x}), u_1^i(2; \mathbf{x}), u_1^i(3; \mathbf{x}), u_1^i(4; \mathbf{x}), u_1^i(6; \mathbf{x}), u_1^i(8; \mathbf{x}), u_1^p(0.5; \mathbf{x}), u_1^p(1; \mathbf{x}), \\ & u_1^p(1.5; \mathbf{x}), u_1^p(2; \mathbf{x}), u_1^p(3; \mathbf{x}), u_1^p(4; \mathbf{x}), u_1^p(6; \mathbf{x}), u_1^p(8; \mathbf{x}), u_1^p(12; \mathbf{x}), u_1^p(14; \mathbf{x})]^T. \end{aligned}$$

This example is based on [18].

Example 3: drug-drug interaction problem

For this example, we consider the case when a patient takes two different drugs. As it is often stated in the instruction for the drug, if two drugs are taken together, they can potentially interact inside the body and can cause an undesirable effect. We model the cases where pitavastatin (for the ease of writing we shall refer to this drug as Drug A) is taken alone or with cyclosporin A (Drug B). The concentration of Drug A is modelled using a mathematical model similar to the Motivating Example and Drug B is modelled using a simplified version of the model. The interaction of Drugs A and B in the liver compartment, when they are administered at the same time is also modelled.

The initial value problem of the mathematical model for Drug A can be written as

$$\frac{d\mathbf{u}}{dt} = \mathbf{g}(\mathbf{u}, t; \mathbf{x}) \quad (38)$$

$$u_i(t=0) = 0 \quad \text{for } i = 1, \dots, 20, \quad (39)$$

$$u_{12} \left(t = \frac{e^{x_{18}}}{2(1+e^{x_{18}})} \right) = 30.4971, \quad (40)$$

$$u_i \left(t = \frac{e^{x_{18}}}{2(1+e^{x_{18}})} \right) = 0 \quad \text{for } i = 1, \dots, 11, 13, \dots, 20. \quad (41)$$

The initial value problem of the mathematical model for Drug A administered with Drug B can be written as:

$$\frac{d\mathbf{u}}{dt} = \mathbf{h}(\mathbf{u}, t; \mathbf{x}) \quad (42)$$

$$u_i(t=0) = 0 \quad \text{for } i = 1, \dots, 33, \quad (43)$$

$$u_{12} \left(t = \frac{e^{x_{18}}}{2(1+e^{x_{18}})} \right) = 30.4971, \quad (44)$$

$$u_{33} \left(t = \frac{e^{x_{19}}}{2(1+e^{x_{19}})} \right) = 2000, \quad (45)$$

$$u_i \left(t = \frac{e^{x_{18}}}{2(1+e^{x_{18}})} \right) = 0 \quad \text{for } i = 1, \dots, 11, 13, \dots, 33, \quad (46)$$

$$u_i \left(t = \frac{e^{x_{19}}}{2(1+e^{x_{19}})} \right) = 0 \quad \text{for } i = 1, \dots, 32. \quad (47)$$

For convenience, we denote the concentration of Drug A at time t when only Drug A is administered as $u_1^A(t; \mathbf{x})$. When both Drugs A and B are administered, we denote the drug concentration of Drug A as $u_1^{AB}(t; \mathbf{x})$ and the concentration of Drug B as $u_{21}^{AB}(t; \mathbf{x})$. For this example, we consider the case where

	Model structure	Parameters to be Estimated	Simulated Observations
Model 1	Three systems of nonlinear ODEs with 20 variables	11 parameters	30 observations
Model 2	Two systems of linear ODEs with 20 variables	11 parameters	22 observations
Model 3	Two systems of nonlinear ODEs with 20 and 33 variables	19 parameters	24 observations

Table 2: Summary of mathematical description of the PBPK models used for the numerical experiments.

the blood sample is taken at $t = 0.5, 1, 1.5, 2, 3, 5, 8, 12$, and for the case where both Drugs A and B are administered, we measure the drug concentration of both drugs. The nonlinear function \mathbf{f} can be written as

$$\mathbf{f}(\mathbf{x}) = [u_1^A(0.5; \mathbf{x}), u_1^A(1; \mathbf{x}), u_1^A(1.5; \mathbf{x}), u_1^A(2; \mathbf{x}), u_1^A(3; \mathbf{x}), u_1^A(5; \mathbf{x}), u_1^A(8; \mathbf{x}), u_1^A(12; \mathbf{x}), u_1^{AB}(0.5; \mathbf{x}), u_1^{AB}(1; \mathbf{x}), u_1^{AB}(1.5; \mathbf{x}), u_1^{AB}(2; \mathbf{x}), u_1^{AB}(3; \mathbf{x}), u_1^{AB}(5; \mathbf{x}), u_1^{AB}(8; \mathbf{x}), u_1^{AB}(12; \mathbf{x}), u_{21}^{AB}(0.5; \mathbf{x}), u_{21}^{AB}(1; \mathbf{x}), u_{21}^{AB}(1.5; \mathbf{x}), u_{21}^{AB}(2; \mathbf{x}), u_{21}^{AB}(3; \mathbf{x}), u_{21}^{AB}(5; \mathbf{x}), u_{21}^{AB}(8; \mathbf{x}), u_{21}^{AB}(12; \mathbf{x})]^T$$

This example is based on [20].

The mathematical description of each PBPK model used for the numerical experiments is summarised in Table 1.

3.1.2 Computation environment

All computational experiments were performed using Matlab 2017a on 3.1 GHz Intel Core i5 processors with MacOS version 10.12.5. The algorithm was written in C++ language and compiled as mex file using clang version 8.1.0. All results of the numerical experiments were summarised and visualised using ggplot2 version 2.2.1 [17] in R version 3.3.2.

3.1.3 Algorithm parameter setting

The initial set of vectors $\{\mathbf{x}_i^{(0)}\}_{i=1}^N$: We generate the initial set of vectors $\{\mathbf{x}_i^{(0)}\}_{i=1}^N$ uniformly randomly in the range of the pharmacologically feasible parameter range based on apriori knowledge (e.g., from the values obtained from the animal experiments or lab experiments).

ODE solver: For Examples 1 and 3 the nonlinear function evaluations require evaluations of stiff systems of ODEs. We use the ODE15s solver [14] with the default setting to evaluate these ODEs. We observed that for some set of parameters, the ODE solver can get stuck in an infinite loop. Here, we set the timeout, where if the ODE evaluation takes longer than 5 seconds, it terminates the evaluation and returns a not-a-number vector.

Levenberg-Marquardt (LM) method: We compare the proposed method with the widely known nonlinear least square solver, Levenberg-Marquardt (LM) method [4], that is implemented in the *lsqcurvefit* function in Matlab. We use each parameter vector in $\{\mathbf{x}_i^{(0)}\}_{i=1}^N$ as the initial estimate and estimate the parameter repeatedly for N times to obtain N set of estimated parameter vectors.

We use LM with default setting as well as set 'FiniteDifferenceStepSize' to be the square root of the default accuracy of the ODE solve (e.g., FiniteDifferenceStepSize = $\sqrt{\text{AbsTol}} = \sqrt{10^{-6}}$). Note that the FiniteDifferenceStepSize of the default setting is 10^{-6} .

Cluster Gauss-Newton (CGN) method: We use the following parameters unless stated otherwise:

$$\lambda_{\text{init}} = 1 \tag{48}$$

$$N = 250. \tag{49}$$

We repeat the iteration for 100 times or until $\lambda_i > 10^{10}$. As can be seen in Equation (23), $\mathbf{x}_i^{(k+1)} \approx \mathbf{x}_i^{(k)}$ for large λ_i , so that we can expect very small update in $\mathbf{x}_i^{(k+1)}$. Hence, in order to mimic the minimum step size stopping criteria, we stop the update and set $\mathbf{x}_i^{(k+1)} = \mathbf{x}_i^{(k)}$ for i where $\lambda_i > 10^{10}$.

3.2 Result: Accuracy

One of the advantages of CGN is that it is more robust against local minima of the nonlinear least squares problem. Hence, we are more likely to obtain the solution of the problem accurately.

From Figures 2-4 we can qualitatively observe that CGN fits the model to the observation at least as well as LM. Figures 3 and 4 show that LM can suffer more from local convergence depending on the initial guess of the parameter compared to CGN.

As can be seen in Figure 5, for Example 1 we observe that CGN finds approximately as many accurate (small SSR) solutions of the nonlinear least squares problem as LM. For Examples 2 and 3, CGN finds more accurate solutions than LM.

In Figure 5, mostly for LM, we can see the step function like behaviour which indicates that LM started from some initial iterates have converged to local minima. On the other hand, especially for Example 2 and 3, we observe that CGN successfully avoid these local minima.

In addition, Figure 5 shows that the final solution we obtain from LM can be sensitive not only to the initial guess but also to the size of the finite difference step if the Jacobian matrix is approximated using finite difference.

For these examples, we were able to adjust the finite element step-size to the theoretical optimal values, as we know the accuracy of the ODE evaluations (cf. LM). However, when the nonlinear function is a complete black box, it would not be possible to adjust the step-size and most likely end up using the default setting (cf. LM def method). As can be seen in Figure 5, without adjusting the step-size, the number of accurate solutions found by the conventional method (LM def) method are consistently less than CGN.

3.3 Result: Computational efficiency (number of nonlinear function evaluations)

Another advantage of CGN is the small number of required nonlinear function evaluations. When solving the nonlinear least squares problem with various initial iterates using conventional methods, it is necessary to solve the problem for each initial iterates one by one. Hence, it is necessary to obtain Jacobian matrix for each time. On the other hand, CGN collectively solves for all the initial iterates, and obtain the linear approximation collectively, resulting in significantly less required number of function evaluations, as can be seen in Figure 6.

3.4 Result: Application to discontinuous nonlinear functions

Obviously, Jacobian based local optimisation methods cannot solve nonlinear least squares problems if the nonlinear function is discontinuous. On the other hand, the Cluster Gauss-Newton (CGN) method uses the linear approximation of the nonlinear function in order to capture the global behaviour of the function. Hence, it does not require the nonlinear function to be continuous.

For the following numerical experiment, we consider the case where the nonlinear function is not continuous to show that CGN can solve nonlinear least squares problem that the conventional Jacobian based method cannot solve. We create such a nonlinear function by rounding the nonlinear function of Example 1 ((28)-(30)) to the first decimal place.

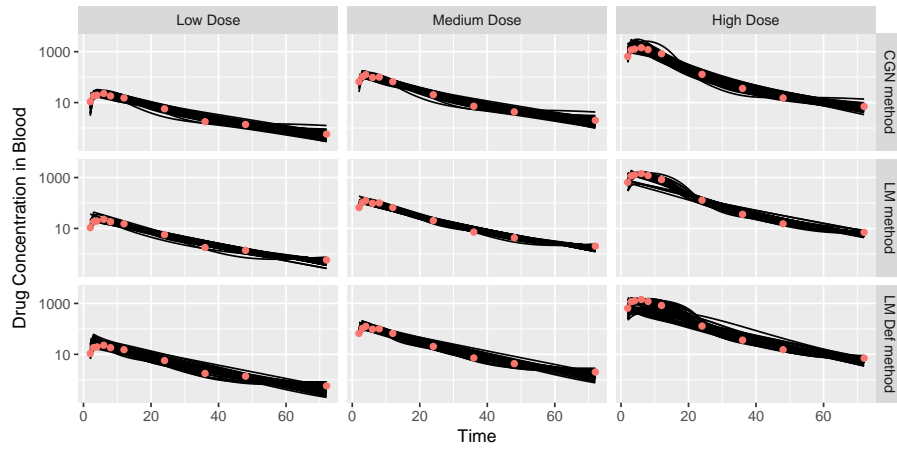


Figure 2: Example 1: Plot of the simulation of drug concentration (black solid line) with observations (red dot). The simulations are based on the set of parameters found by each method whose SSR are within the 200 best fit (out of 250) for each method. CGN method: Cluster Gauss-Newton method, LM method: Levenberg-Marquardt method, LM Def method: Levenberg-Marquardt method with default setting.

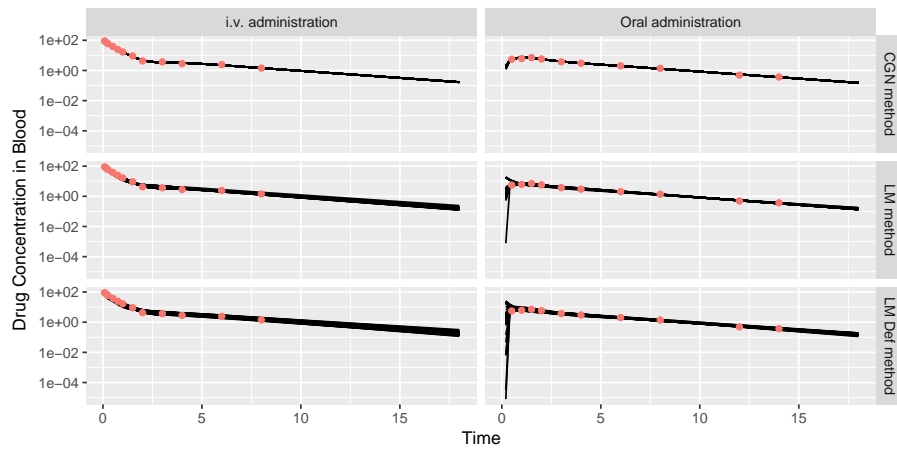


Figure 3: Example 2: Plot of the simulation of drug concentration (black solid line) with observations (red dot). The simulations are based on the set of parameters found by each method whose SSR are within the 200 best fit (out of 250) for each method.

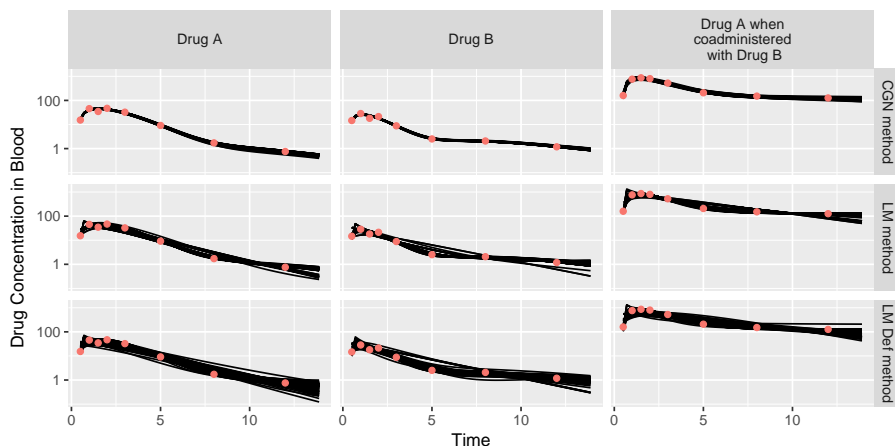


Figure 4: Example 3: Plot of the simulation of drug concentration (black solid line) with observations (red dot). The simulations are based on the set of parameters found by each method whose SSR are within the 200 best fit (out of 250) for each method.

As can be seen in Figure 7, the CGN method was able to fit the model appropriately to the observation while LM was unable to find suitable model parameters.

4 Concluding Remarks

We have proposed the Cluster Gauss-Newton (CGN) method, a new computational method for obtaining multiple solutions of a **nonlinear least squares problem**. Considering that our previously developed Cluster Newton method can only solve an underdetermined **system of nonlinear equations**, the proposed algorithm has a significantly broader range of applications for parameter estimation problems.

The development of this algorithm was motivated by the parameter estimation problem that appears in the field of pharmaceutical drug development. The particular nature of the model, where the model is over parameterised, and consideration of multiple possible parameters is necessary, motivated us to develop a new computational method. The fact that our algorithm obtains multiple solutions collectively has made it significantly more computationally efficient and robust against convergence to local minima, compared to repeatedly solving the least squares problem using the standard Levenberg-Marquardt method. We have demonstrated these advantages of the proposed method using three examples that come from the real world drug development projects. Based on this experience, we have identified many potential use cases of this algorithm among pharmaceutical scientists, so we have created a graphical user interface based software which is available at http://www.bluetree.me/CGNmethod_for_PBPKmodels.

By minimising the assumption on the nonlinear function, where it can be a “black box” or even non-differentiable, we have ensured the ease of use for those who may not have a substantial background in mathematics or scientific computing. We believe this advantage of the proposed method will be appreciated by potential users of the algorithm in industry. In this paper, we have used the pharmacokinetics models as examples. However, as we do not assume any particular form of the nonlinear function, we believe the proposed method can be used for many other mathematical models in various scientific fields. We note that there are existing derivative-free methods for nonlinear least-squares problems such as [21, 5]. However, our CGN is unique in the sense that it was developed to obtain multiple solutions.

Although we have paid significant attention to the usefulness of the algorithm for industrial applications, the unique mathematical properties such as speed of convergence as well as robustness against converging to local minima can be of mathematical interest. Further investigations on the theoretical convergence as well as the refinement of the regularisation strategy of the algorithm are left for future research.

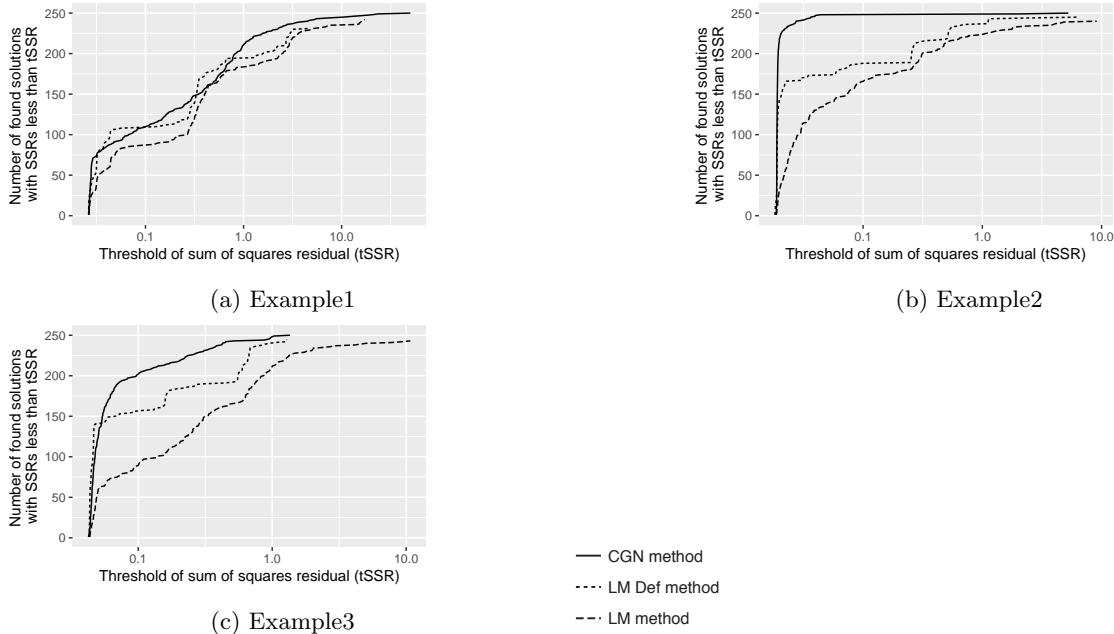


Figure 5: Number of solutions found by the various methods for given accuracy threshold (tSSR). Smaller SSR indicates more accurate solution to the nonlinear-least squares problem. CGN method (solid line): Cluster Gauss-Newton method, LM method: Levenberg-Marquardt method, LM Def method: Levenberg-Marquardt method with default setting.

5 Acknowledgement

We would like to thank Professor Akihiko Konagaya for giving us the opportunity to initiate this research.

A Motivating Example

In this appendix, we introduce a motivating example to illustrate how the proposed method can be used in real life. We consider a fictitious scenario where a newly developed drug is tested for the first time in a human. Before the drug is given to a human, the biochemical properties of the drug are studied in-test-tube (in-vitro) and in-animal experiments. However, how the drug behaves in the human body is still uncertain. Based on the results of in-vitro and in-animal experiments, the team has decided that 100mg is a safe amount of the drug to be given to a human and the experiment is conducted with a healthy normal volunteer, and the drug concentration in blood plasma is measured throughout time. Using these measurements, we estimate the multiple possible model parameters which can be used to simulate various scenarios. The following workflow can be envisioned:

1: Construct a mathematical model based on the understanding of the physiology and biochemical properties of the drug.

In this example, we use the model presented in [16]. The mathematical model is depicted in Figure 8, and it can be written as a system of nonlinear ordinary differential equations with 20 variables. There are two types of model parameters in this model: physiological parameters and kinetic parameters. Examples of the physiological parameters are the sizes of the organs or the blood flow rates between the organs. As the human physiology is well studied and these parameters usually do not depend on the drugs, we can assume these parameters to be known. The kinetic parameters, such as, how fast the drug gets excreted from the body or how easily it binds to tissues are the parameters that depend on the drug and usually is not very well

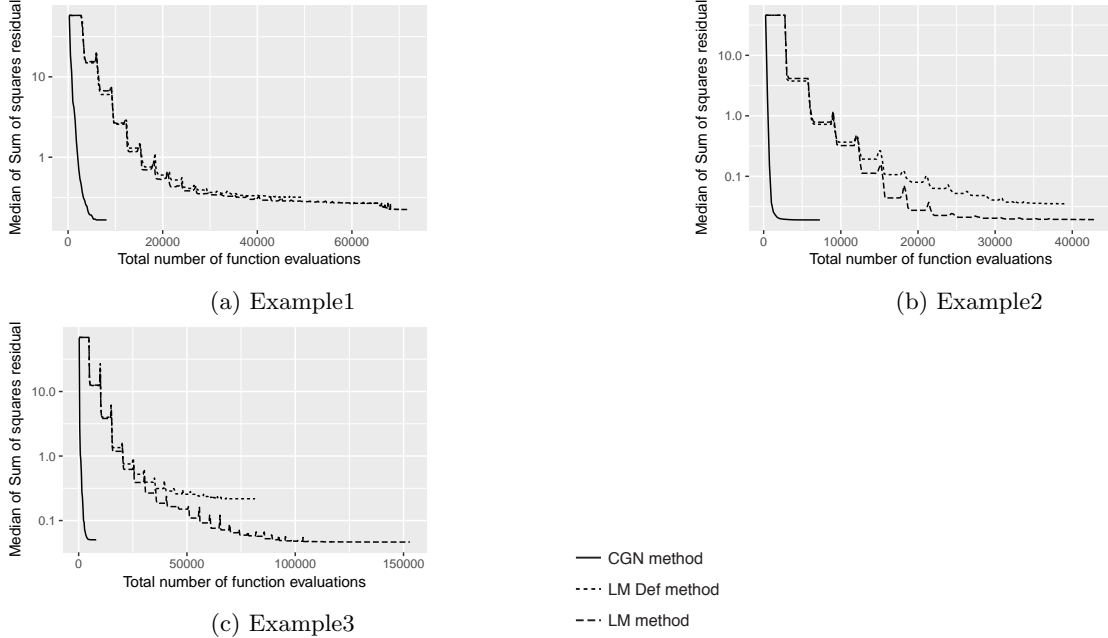


Figure 6: Reduction of the median of sum of squares residual as the number of function evaluations. As each function evaluation involves solving a system of ODEs numerically, the computational cost is approximately proportional to the number of function evaluations. CGN method: Cluster Gauss-Newton method, LM method: Levenberg-Marquardt method, LM Def method: Levenberg-Marquardt method with default setting.

known. Before the first in-human experiment, the drug development team characterises these parameters using an organ in test-tubes or by administering the drug to an animal. However, these parameters can differ from animal to human, so we do not have a very accurate estimate of these parameters. The differences in these parameters between a human and an animal can be several orders of magnitude. Figure 9 depicts plots of the drug concentration simulation where the kinetic parameters are sampled within a reasonable range of the parameters. As can be seen in Figure 9, we cannot obtain any useful information just by randomly sampling the kinetic parameters from the feasible range.

2: Sample multiple possible model parameter sets that fit the model prediction of the drug concentration to the observed data from the 100mg experiment. We now use the observed data from the experiment where 100mg of the drug was given to a human. The red dots in Figure 10 depict the observed data. The left panel of Figure 10 shows some of the simulation results using the parameter sets of the initial iterate of CGN. The right panel of Figure 10 shows some of the simulation results after 20 iterations of CGN. As can be seen in Figure 10, CGN can find multiple sets of parameters that fit the observed data. The parameter values are depicted in the box plots in Figure 11. As can be seen in Figure 11, after 20 iterations of CGN, the distribution of some of the parameters shrinks significantly suggesting these parameters can be identified from the observations while the distribution of some of the parameters are unchanged indicating that these parameters cannot be identified from the observation. In Figure 12, we have plotted scatter plots of the parameters found by CGN. As can be seen in Figure 12, even if the parameter cannot be identified from the observation, some nonlinear relationships can occasionally be identified between the parameters.

B Relation with previous work

We initially proposed the Cluster Newton (CN) method for sampling multiple solutions of a system of nonlinear equations where the number of unknowns is more than number of observations [1, 2, 7].

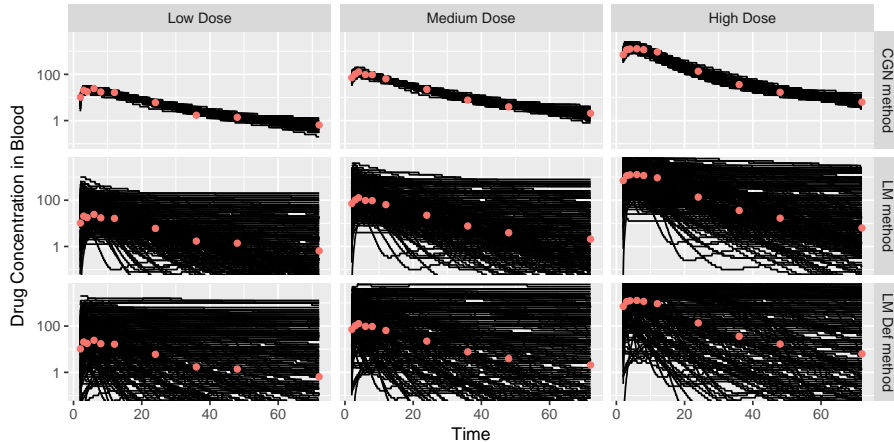


Figure 7: Example 1 when the nonlinear function is rounded to one decimal place: Plot of the simulation of drug concentration (black solid line) with observations (red dot). The simulations are based on the set of parameters found by each method whose SSR are within the 200 best fit (out of 250) for each method. Notice that the simulation result is not smooth representing the fact the $u_1(t; \mathbf{x})$ is rounded to the first decimal place resulting in the nonlinear function \mathbf{f} to become discontinuous.

The parameter fitting problems presented in [19, 15, 10] uses CN to fit complex PBPK models to the drug (and its metabolite) concentration measurements over time. As the drug concentration was measured repeatedly from the patient, there is a larger number of observations than the number of unknown parameters. CN assumes an underdetermined problem, where the number of observations is less than the number of parameters. To use CN, in [19, 15, 10], the authors constructed a summary value called Area Under the time-concentration Curve (AUC) to reduce the number of observations and fit the model to the summary value using CN. The AUC is essentially the time integral of the drug concentration from the time drug is administered to infinity. After finding multiple possible parameters that match the AUC of the model and the observations, Yoshida et al. and Toshimoto et al. [19, 15] selected the parameter sets that fit the time-course drug concentrations reasonably well from these parameter sets found using CN. Kim et al. [10] used a parameter set obtained using CN as the initial iterate for the Levenberg-Marquardt method and fitted the model to the time-course drug concentration data.

Based on the current use of CN, we have identified two bottlenecks of the workflow employed in [19, 15, 10]. Firstly, CN solves a system of underdetermined system of nonlinear **equations**. Hence, the model needs to be constructed in a way that the observation and the model prediction match **exactly**. Hence, if there is a model misspecification or significant measurement error that influence the summary values (e.g. AUC) sufficiently so that there is no model prediction that exactly matches the observation derived summary value, then CN breaks down.

Secondly, in order to obtain the parameter sets that reasonably fit the original data (e.g., time-course concentration data), we need to obtain many parameter sets that fit the summary values (e.g., AUC). This is simply because we need to randomly sample from (number of parameters)-(number of summary values) dimension space to obtain the desired parameter sets. As a result, [15] had to find 500 000 parameter sets that fit the summary value (AUC) using CN and then was able to obtain 30 parameter sets that reasonably fit the original data (time-course drug concentration).

To overcome these bottlenecks, we have suggested these authors to formulate these parameter estimation problems as nonlinear least squares problem and we have created the Cluster Gauss-Newton method (CGN). The new method efficiently obtains multiple possible parameters by solving a nonlinear least squares problem so that the method does not break down even if the model does not exactly match the observation. Also, the new algorithm does not require the number of observations to be less than the number of parameters so that there is no need to summarise the observation and can directly use the original observations (e.g.,

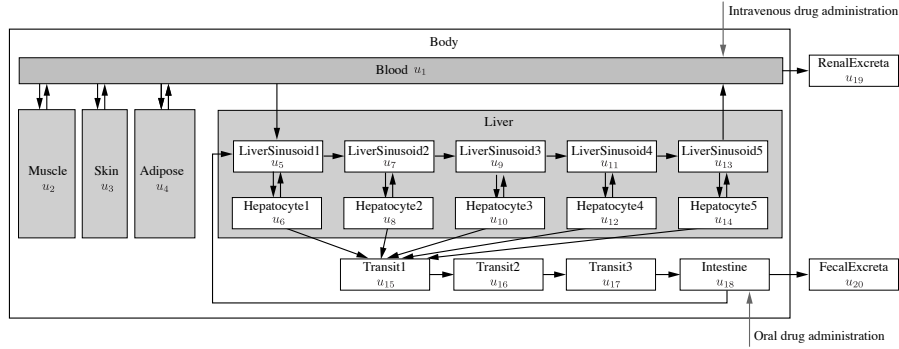


Figure 8: A schematic diagram of a physiologically based pharmacokinetic model. (Arrows represent the movement of the drug to a different part of the body. Variables u_i are the drug concentration or the amount of the drug in each compartment. The body is divided into Blood, Muscle, Skin, Adipose, Liver and Intestine. The liver is further divided into ten compartments to model the complex drug behaviour in the liver. The intestine is divided into four compartments, three transit compartments and one intestine compartment, to model the time it takes for the drug to reach the intestine.)

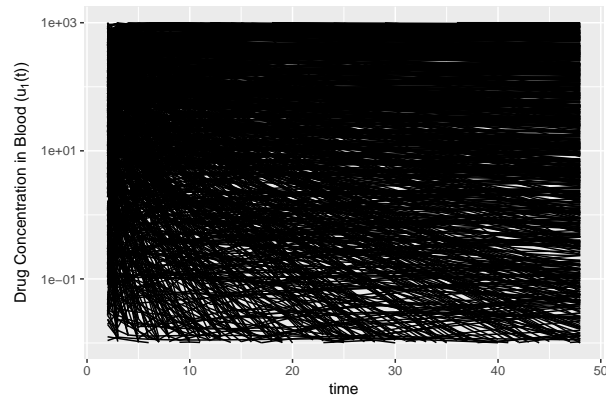


Figure 9: Simulation of the drug concentration in blood plasma using the parameters that are naively sampled from the range of possible kinetic parameters. Note that these simulations do not give any useful information.

time-course concentration measurements). As can be seen in Figure 13, the new algorithm enables us to sample multiple possible parameters significantly more accurately than the approach using CN.

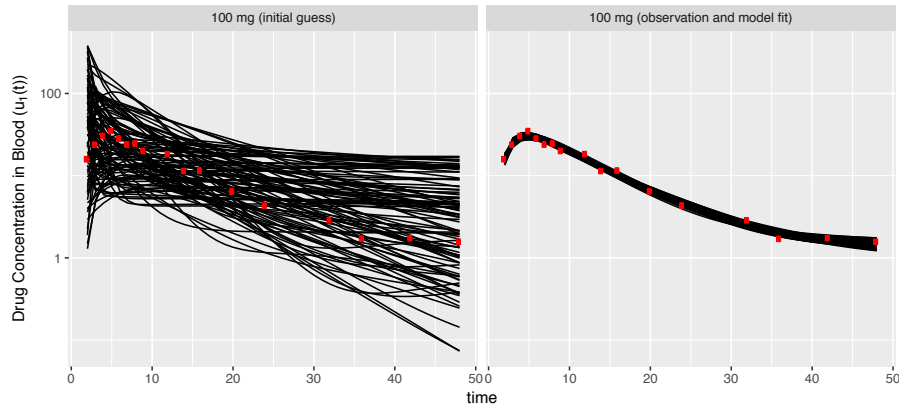


Figure 10: Plot of the simulation of drug concentration (black solid line) with observations (red dot). Simulation results are based on the parameters for the initial iterate for CGN and the parameters found after 20 iterations of CGN. In the left panel, the simulation results based on the top 100 sets of the parameters (out of 1000 parameter sets in the cluster) from the initial cluster are shown. In the right panel, the simulation results based on the top 100 sets of the parameters (out of 1000 parameter sets in the cluster) after 20 iterations of CGN are shown.

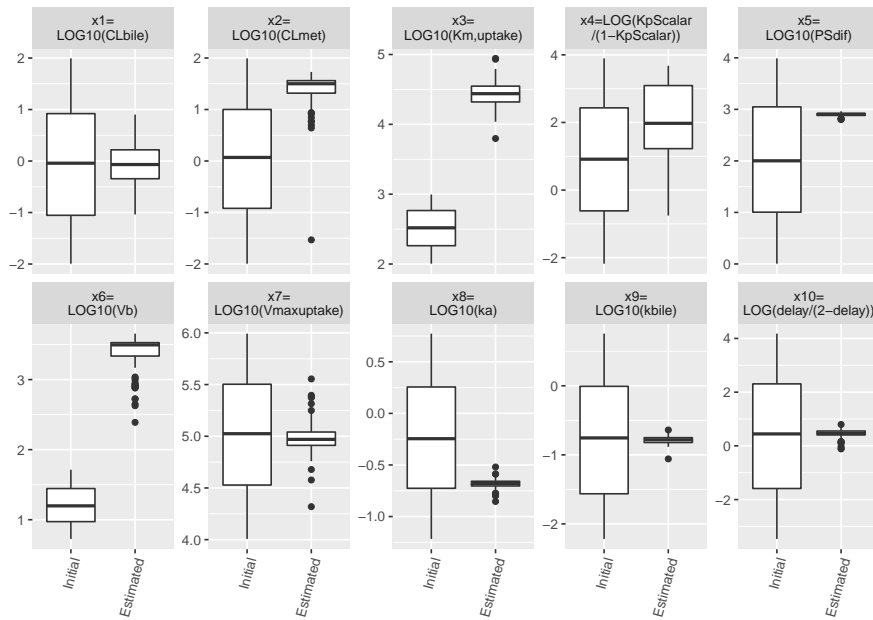


Figure 11: Box plots of top 100 parameters (parameters whose corresponding SSR is the least 100 within the cluster) from the initial cluster (left) and the cluster after 20 iterations of CGN (right). Note the distributions of x_5, x_8, x_9, x_{10} clearly shrunk after 20 iterations while the distribution of x_4 did not change noticeably. (Box plot: The edges of the boxes are the 75th and 25th percentiles. The line in the box is the median, and the whiskers extend to the largest and the smallest value within the 1.5 times the inter-quartile range. Dots are the outliers outside the whiskers.)

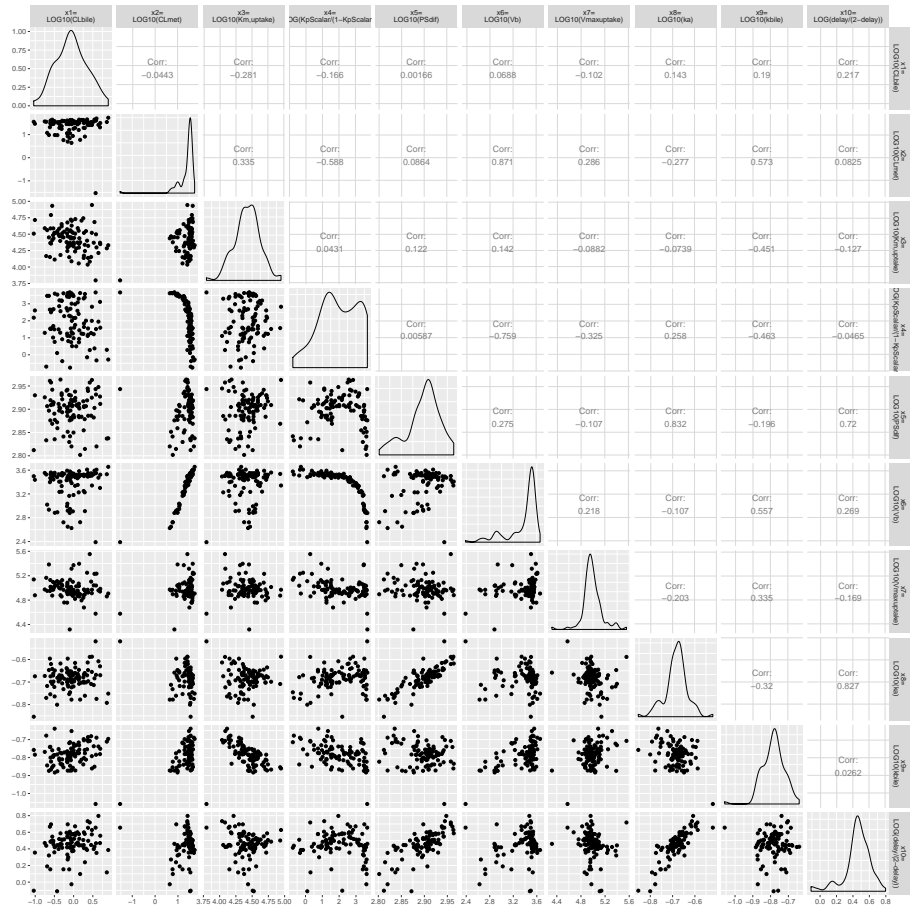


Figure 12: Scatter plots of parameters. As can be seen in this example, we can find parameter-parameter correlations of some of the parameters found by CGN.

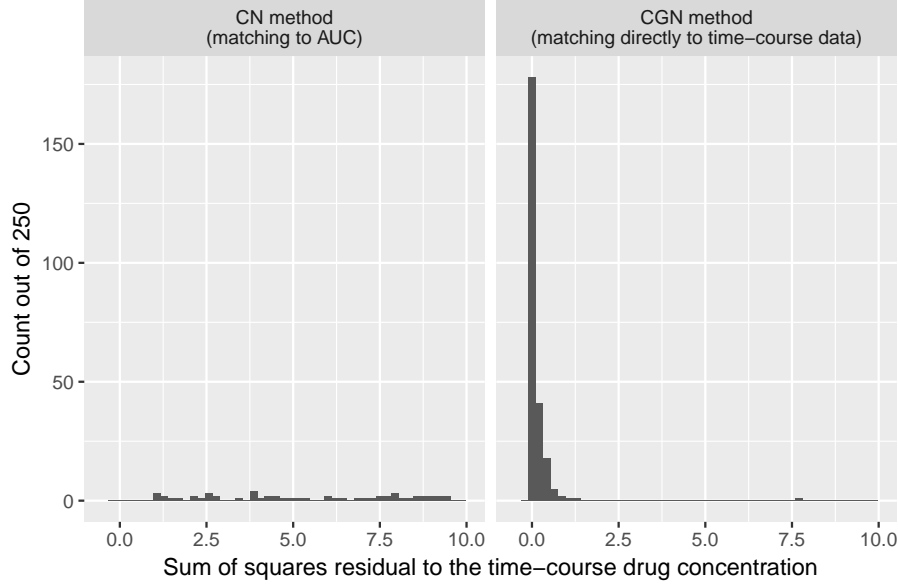


Figure 13: Comparison of the accuracy of the model fit of the Motivating Example (cf. Appendix A) using the approach employed in [19, 15] using the Cluster Newton (CN) method and the proposed Cluster Gauss-Newton (CGN) method.

C Derivation of equation (19)

From equation (16) we have

$$\begin{aligned}
A_{(i)}^{(k)} &= \operatorname{argmin}_{A \in \mathbb{R}^{m \times n}} \sum_{j=1}^N \left(d_{j(i)}^{(k)} \left\| \Delta \mathbf{y}_{j(i)}^{(k)} - A \Delta \mathbf{x}_{j(i)}^{(k)} \right\|_2 \right)^2, \\
&= \operatorname{argmin}_{A \in \mathbb{R}^{m \times n}} \sum_{j=1}^N \left\| d_{j(i)}^{(k)} \left(A \Delta \mathbf{x}_{j(i)}^{(k)} - \Delta \mathbf{y}_{j(i)}^{(k)} \right) \right\|_2^2, \\
&= \operatorname{argmin}_{A \in \mathbb{R}^{m \times n}} \left\| \left(A \Delta X_{(i)}^{(k)} - \Delta Y_{(i)}^{(k)} \right) D_{(i)}^{(k)} \right\|_F^2, \\
&= \operatorname{argmin}_{A \in \mathbb{R}^{m \times n}} \left\| D_{(i)}^{(k)} \left(\Delta X_{(i)}^{(k)T} A^T - \Delta Y_{(i)}^{(k)T} \right) \right\|_F^2,
\end{aligned} \tag{50}$$

where $\|B\|_F = \left(\sum_{i=1}^m \sum_{j=1}^n b_{ij}^2 \right)^{\frac{1}{2}}$ is the Frobenius norm of the matrix $B = (b_{ij}) \in \mathbb{R}^{m \times n}$.

Let $A_{(i)}^{(k)T} = \left[\boldsymbol{\alpha}_{1(i)}^{(k)}, \dots, \boldsymbol{\alpha}_{m(i)}^{(k)} \right] \in \mathbb{R}^{n \times m}$, where $\boldsymbol{\alpha}_{j(i)}^{(k)} \in \mathbb{R}^n$ for $j = 1, \dots, m$, and $\Delta Y_{(i)}^{(k)T} = \left[\Delta \boldsymbol{\eta}_{1(i)}^{(k)}, \Delta \boldsymbol{\eta}_{2(i)}^{(k)}, \dots, \Delta \boldsymbol{\eta}_{m(i)}^{(k)} \right] \in \mathbb{R}^{N \times m}$, where $\Delta \boldsymbol{\eta}_{j(i)}^{(k)} \in \mathbb{R}^N$, for $j = 1, \dots, m$. Then, equation (50) is equivalent to

$$\boldsymbol{\alpha}_{j(i)}^{(k)} = \operatorname{argmin}_{\boldsymbol{\alpha} \in \mathbb{R}^n} \left\| D_{(i)}^{(k)} \left(\Delta X_{(i)}^{(k)T} \boldsymbol{\alpha} - \Delta \boldsymbol{\eta}_{j(i)}^{(k)} \right) \right\|_2 \quad j = 1, \dots, m, \tag{51}$$

which is equivalent to equation (19).

Note that equation (50) is equivalent to the normal equations

$$\Delta X_{(i)}^{(k)} D_{(i)}^{(k)2} \Delta X_{(i)}^{(k)T} A_{(i)}^{(k)T} = \Delta X_{(i)}^{(k)} D_{(i)}^{(k)2} \Delta Y_{(i)}^{(k)T}, \tag{52}$$



Figure 14: Number of solutions found for given accuracy threshold (tSSR) using various weights for the linear approximation (i.e., various γ). Smaller SSR indicates more accurate solution to the nonlinear-least squares problem.

and equation (51) is equivalent to the normal equations

$$\Delta X_{(i)}^{(k)} D_{(i)}^{(k)2} \Delta X_{(i)}^{(k)T} \alpha_{j(i)}^{(k)} = \Delta X_{(i)}^{(k)} D_{(i)}^{(k)2} \Delta \eta_{j(i)}^{(k)} \quad j = 1, \dots, m. \quad (53)$$

D Numerical experiments on the influence of the weight of the linear approximation

To illustrate the influence of the weight $d_{j(i)}^{(k)}$ for the weighted linear approximation in 2-1 of the algorithm, we conducted numerical experiments using Example 1. For this numerical experiment, we varied the parameter $\gamma \geq 0$ in equation (22):

$$d_{j(i)}^{(k)} = \begin{cases} \left(\frac{1}{\sum_{l=1}^n ((x_{lj}^{(k)} - x_{li}^{(k)}) / (x_l^U - x_l^L))^2} \right)^\gamma & \text{if } j \neq i \\ 0 & \text{if } j = i \end{cases}. \quad (54)$$

In Figure 14, we show the number of solutions found by CGN for given accuracy threshold. In Figure 15, we show the convergence plot of SSR. As can be seen from Figures 14 and 15, the weight for the linear approximation improves the accuracy and the speed of CGN. Note that $\gamma = 0$, which corresponds to giving equal weights to all the cluster points is not optimal. In this example, $\gamma = 2$ gave the best result.

E Numerical experiments on the influence of the regularisation

To illustrate the necessity and the influence of the regularisation in 2-2 of the algorithm, we conducted numerical experiments using Example 1. We varied the initial value of the regularisation coefficient λ_{init} and tested CGN. In Figure 16, we show the number of solutions found by CGN for given accuracy threshold. In Figure 17, we show the convergence of SSR. As can be seen from Figures 16 and 17, the regularisation is necessary for CGN to perform well. For this example, $\lambda_{\text{init}} = 0.1$ gave the best result.

F ODE expressions of the PBPk model used as the motivating example

In this subsection we explicitly write out the mathematical model used in the motivating example in Appendix A as a system of ODEs. The other PBPk models used in this paper can be similarly written as a

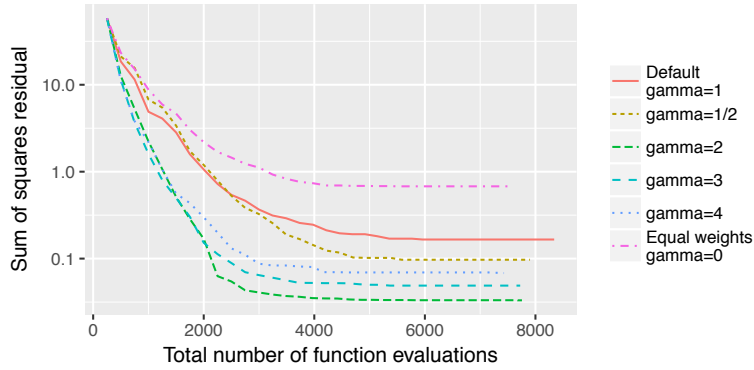


Figure 15: Reduction of the median of sum of squares residual as the number of function evaluations with various weights for the linear approximation (i.e., various γ). As each function evaluation involves solving a system of ODEs numerically, the computational cost is approximately proportional to the number of function evaluations.

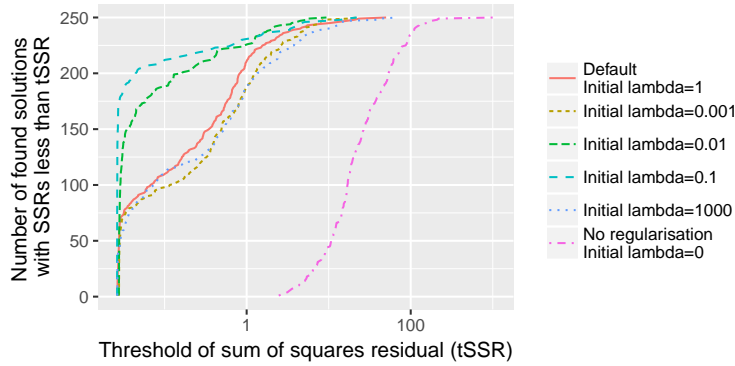


Figure 16: Number of solutions found for given accuracy threshold (tSSR) using various initial lambda (λ_{init}). Smaller SSR indicates more accurate solution to the nonlinear-least squares problem.

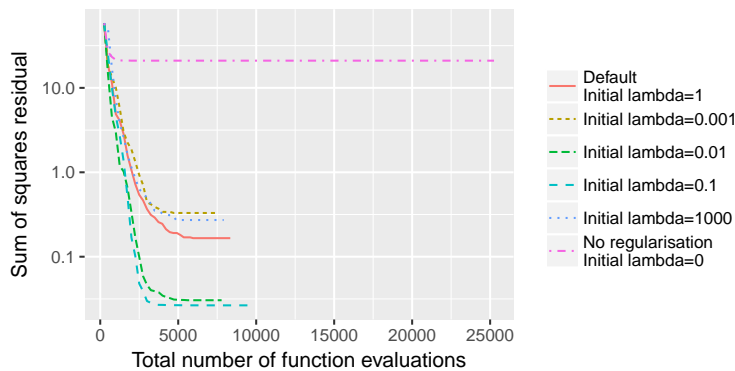


Figure 17: Reduction of the median of sum of squares residual as the number of function evaluations with various initial lambda (λ_{init}). As each function evaluation involves solving a system of ODEs numerically, the computational cost is approximately proportional to the number of function evaluations.

system of ODEs. For the model parameters appearing in these ODEs, we follow the usual notations used in pharmacokinetics and we will provide brief descriptions of these parameters. For more detailed description of these parameters, we refer the reader to the standard textbooks in pharmacokinetics (e.g., [12]).

ODE for the blood compartment

$$\frac{du_1}{dt} = \frac{Q_h(u_{13} - u_1) - CL_r u_1 - Q_m(u_1 - \frac{u_2}{Kp_m Kp_{scalar}}) - Q_s(u_1 - \frac{u_3}{Kp_s Kp_{scalar}}) - \frac{Q_a(u_1 - \frac{u_4}{Kp_a Kp_{scalar}})}{V_b}}{V_b}$$

Q_h is the blood flow rate through the liver. The unit is typically L/hr.

CL_r is the rate of the drug being excreted as urine. The unit is typically L/hr.

V_b is the volume of the blood compartment. The unit is typically L.

Q_m, Q_s, Q_a are the blood flow rates to muscle, skin, and adipose, respectively. The unit is typically L/hr.

V_m, V_s, V_a are the volumes of muscle, skin, and adipose compartments, respectively. The unit is typically L.

Kp_m, Kp_s, Kp_a are the partition coefficients of the drug for the muscle, skin and adipose, respectively.

The partition coefficient is the ratio between the drug concentration in the blood plasma and the tissue at equilibrium when the tissue is in contact with the blood. We usually assume that these values can be measured by *in-vitro* experiments. Hence, they are usually fixed parameters in the model.

Kp_{scalar} is a scaling factor for the partitioning.

ODE for the muscle compartment

$$\frac{du_2}{dt} = \frac{Q_m}{V_m} \left(u_1 - \frac{1}{Kp_m Kp_{scalar}} u_2 \right) \quad (55)$$

ODE for the skin compartment

$$\frac{du_3}{dt} = \frac{Q_s}{V_s} \left(u_1 - \frac{1}{Kp_s Kp_{scalar}} u_3 \right) \quad (56)$$

ODE for the adipose (fat) compartment

$$\frac{du_4}{dt} = \frac{Q_a}{V_a} \left(u_1 - \frac{1}{Kp_a Kp_{scalar}} u_4 \right) \quad (57)$$

ODEs for the liver compartments

For a compartment representing the blood vessel in the liver (Liver Sinusoid 1)

$$\frac{du_5}{dt} = -\frac{V_{\max_{\text{uptake}}} + f_b PS_{\text{dif}}}{V_{hc}} u_5 + \frac{f_h PS_{\text{dif}}}{V_{hc}} u_6 + \frac{Q_h(u_1 - u_5) + ka u_{18}}{\frac{V_{hc}}{5}} \quad (58)$$

ka is the rate of the drug being absorbed from the intestines and transported to the liver through the portal vein. The unit is typically L/hr.

V_{hc} is the volume of the blood in blood vessel.

PS_{dif} is the diffusion constant between the liver sinusoid compartment and the hepatocyte compartment.

f_b is the ratio of the drug that is not bound to the protein in blood in the blood vessel in the liver.

f_h is the ratio of the drug that is not bound to the protein in the liver cells. Only the portion of the drug that is not bound to the protein can permeate in and out of the liver cells.

For compartments representing the blood vessel in the liver (Liver Sinusoid 2, 3, 4, 5)

$$\frac{du_{7+2i}}{dt} = -\frac{V_{\max_{\text{uptake}}} + f_b PS_{\text{dif}}}{V_{hc}} u_{7+2i} + \frac{f_h PS_{\text{dif}}}{V_{hc}} u_{8+2i} + \frac{Q_h(u_{5+2i} - u_{7+2i})}{\frac{V_{hc}}{5}}$$

for $i = 0, 1, 2, 3$.

$V_{\max_{\text{uptake}}}$ and Km_{uptake} are constants for the Michaelis-Menten kinetics where the active uptake of the drug from the blood to the liver cells by membrane transport protein (also known as ‘‘transporter’’).

Compartments representing liver cells (Hepatocyte 1, 2, 3, 4, 5)

$$\frac{du_{6+2i}}{dt} = \frac{V_{\max_{\text{uptake}}}}{Km_{\text{uptake}} + u_{5+2i}} + f_b PS_{\text{dif}} - \frac{f_h(PS_{\text{dif}} + (CL_{\text{met}} + CL_{\text{bile}}))}{V_{he}} u_{6+2i}$$

for $i = 0, 1, 2, 3, 4$.

V_{he} is the volume of liver cells.

ODE for the transit compartment 1

$$\frac{du_{15}}{dt} = f_h CL_{\text{bile}} \frac{u_6 + u_8 + u_{10} + u_{12} + u_{14}}{5} - k_{\text{bile}} u_{15} \quad (59)$$

u_{15} is the amount of the drug in the transit compartment 1. Transit compartment can be thought of as a fictitious compartment that introduces the delay of the drug delivery to to the intestines. CL_{met} is a clearance (speed that drug is cleared out) due to the metabolisation of the drug of the subject. The unit is typically L/hr.

CL_{bile} is a clearance due to the biliary excretion of the drug of the subject. The unit is typically L/hr.

k_{bile} is a diffusion coefficient between the transit compartments. The unit is typically 1/hr.

f_h is the fraction of the drug cleared by liver, it is typically unit-less.

ODE for the transit compartment 2

$$\frac{du_{16}}{dt} = k_{\text{bile}} (u_{15} - u_{16}) \quad (60)$$

u_{16} is the amount of the drug in the transit compartment 2. k_{bile} is a diffusion constant where the drug is diffused into bile, the unit is typically 1/hr.

ODE for the transit compartment 3

$$\frac{du_{17}}{dt} = k_{\text{bile}} (u_{16} - u_{17}) \quad (61)$$

u_{17} is the amount of the drug in the transit compartment 3.

ODE for the intestine compartment

$$\frac{du_{18}}{dt} = k_{\text{bile}} u_{17} - \frac{ka}{FaFg} u_{18} \quad (62)$$

u_{18} is the amount of the drug in the intestine. $FaFg$ is the fraction of the drug that gets absorbed by the intestines.

G Re-parameterisation

For the mathematical model we have introduced in Appendix F, some of the parameters may be known for the drug of interest. For the motivating example presented in Appendix A, we have assumed the following parameters to be known:

$$CL_r = 0, \quad FaFg = 0.55, \quad Kp_a = 0.086, \quad Kp_m = 0.113 \quad (63)$$

$$Kp_s = 0.478, \quad Q_a = 15.61, \quad Q_h = 86.94, \quad Q_m = 44.94 \quad (64)$$

$$Q_s = 17.99, \quad V_a = 10.01, \quad V_{hc} = 1.218, \quad V_{he} = 0.469 \quad (65)$$

$$V_m = 30.03, \quad V_s = 7.77, \quad f_b = 0.00617, \quad f_h = 0.012 \quad (66)$$

Also, most of the parameters have known physiologically or chemically possible range (e.g., clearances cannot be negative). Thus for those parameters, we re-parameterise to impose known constraints. For the motivating example presented in Appendix A, we have re-parameterised as in the followings:

$$CL_{\text{bile}} = 10^{x_1}, \quad CL_{\text{met}} = 10^{x_2}, \quad Km_{\text{uptake}} = 10^{x_3}, \quad (67)$$

$$Kp_{\text{Scalar}} = \frac{e^{x_4}}{1 + e^{x_4}} \quad PSdif = 10^{x_5}, \quad Vb = 10^{x_6}, \quad (68)$$

$$Vmax_{\text{uptake}} = 10^{x_7}, \quad ka = 10^{x_8} \quad k_{\text{bile}} = 10^{x_9}. \quad (69)$$

References

- [1] Y. AOKI, K. HAYAMI, H. DE STERCK, AND A. KONAGAYA, *Cluster newton method for sampling multiple solutions of an underdetermined inverse problem: Parameter identification for pharmacokinetics*, NII Technical Reports, (2011), pp. 1–38.
- [2] Y. AOKI, K. HAYAMI, H. DE STERCK, AND A. KONAGAYA, *Cluster Newton method for sampling multiple solutions of underdetermined inverse problems: Application to a parameter identification problem in pharmacokinetics*, SIAM Journal on Scientific Computing, 36 (2014), pp. B14–B44, <https://doi.org/10.1137/120885462>.
- [3] S. ASAMI, D. KIGA, AND A. KONAGAYA, *Constraint-based perturbation analysis with cluster Newton method: A case study of personalized parameter estimations with irinotecan whole-body physiologically based pharmacokinetic model*, BMC Systems Biology, (2017), <https://doi.org/10.1186/s12918-017-0513-2>.
- [4] Å. BJÖRCK, *Numerical Methods for Least Squares Problems*, SIAM, 1996, <https://doi.org/10.1137/1.9781611971484>.
- [5] C. CARTIS AND L. ROBERTS, *A derivative-free gauss-newton method*, arXiv preprint arXiv:1710.11005, (2017).
- [6] Y. FUKUCHI, K. TOSHIMOTO, T. MORI, K. KAKIMOTO, Y. TOBE, T. SAWADA, R. ASAUMI, T. IWATA, Y. HASHIMOTO, K. ICHI NUNOYA, H. IMAWAKA, S. MIYAUCHI, AND Y. SUGIYAMA, *Analysis of Nonlinear Pharmacokinetics of a Highly Albumin-Bound Compound: Contribution of Albumin-Mediated Hepatic Uptake Mechanism*, Journal of Pharmaceutical Sciences, (2017), <https://doi.org/10.1016/j.xphs.2017.04.052>.
- [7] P. GAUDREAU, K. HAYAMI, Y. AOKI, H. SAFOUHI, AND A. KONAGAYA, *Improvements to the cluster Newton method for underdetermined inverse problems*, Journal of Computational and Applied Mathematics, 283 (2015), pp. 122–141, <https://doi.org/10.1016/j.cam.2015.01.014>.
- [8] P. C. HANSEN, *Rank-deficient and discrete ill-posed problems: numerical aspects of linear inversion*, vol. 4, SIAM, 2005.
- [9] K. HAYAMI, *Convergence of the conjugate gradient method on singular systems*, NII Technical Reports, (2018), pp. 1–7, also available in arXiv 1809.00793, 2018.
- [10] S.-J. KIM, K. TOSHIMOTO, Y. YAO, T. YOSHIKADO, AND Y. SUGIYAMA, *Quantitative Analysis of Complex Drug-Drug Interactions Between Repaglinide and Cyclosporin A/Gemfibrozil Using Physiologically Based Pharmacokinetic Models With In Vitro Transporter/Enzyme Inhibition Data*, Journal of Pharmaceutical Sciences, (2017), <https://doi.org/10.1016/j.xphs.2017.04.063>, <http://linkinghub.elsevier.com/retrieve/pii/S0022354917303337>.

- [11] T. NAKAMURA, K. TOSHIMOTO, W. LEE, C. K. IMAMURA, Y. TANIGAWARA, AND Y. SUGIYAMA, *Application of PBPK Modeling and Virtual Clinical Study Approaches to Predict the Outcomes of CYP2D6 Genotype-Guided Dosing of Tamoxifen*, CPT: Pharmacometrics & Systems Pharmacology, (2018), <https://doi.org/10.1002/psp4.12307>, <http://doi.wiley.com/10.1002/psp4.12307>.
- [12] M. ROWLAND, T. N. TOZER, H. DERENDORF, AND G. HOCHHAUS, *Clinical pharmacokinetics and pharmacodynamics: concepts and applications*, Wolters Kluwer Health/Lippincott William & Wilkins Philadelphia, PA, 2011.
- [13] Y. SAAD, *Iterative Methods for Sparse Linear Systems, Second Ed.*, SIAM, 2003.
- [14] L. F. SHAMPINE AND M. W. REICHEL, *The MATLAB ODE Suite*, SIAM Journal on Scientific Computing, (1997), <https://doi.org/10.1137/S1064827594276424>.
- [15] K. TOSHIMOTO, A. TOMARU, M. HOSOKAWA, AND Y. SUGIYAMA, *Virtual Clinical Studies to Examine the Probability Distribution of the AUC at Target Tissues Using Physiologically-Based Pharmacokinetic Modeling: Application to Analyses of the Effect of Genetic Polymorphism of Enzymes and Transporters on Irinotecan Ind*, *Pharmaceutical Research*, 34 (2017), pp. 1584–1600, <https://doi.org/10.1007/s11095-017-2153-z>, <http://link.springer.com/10.1007/s11095-017-2153-z>.
- [16] T. WATANABE, H. KUSUHARA, K. MAEDA, Y. SHITARA, AND Y. SUGIYAMA, *Physiologically Based Pharmacokinetic Modeling to Predict Transporter-Mediated Clearance and Distribution of Pravastatin in Humans*, *Journal of Pharmacology and Experimental Therapeutics*, (2009), <https://doi.org/10.1124/jpet.108.146647>.
- [17] H. WICKHAM, *ggplot2: Elegant Graphics for Data Analysis*, Springer-Verlag New York, 2016, <http://ggplot2.org>.
- [18] Y. YAO, K. TOSHIMOTO, S.-J. KIM, T. YOSHIKADO, AND Y. SUGIYAMA, *Quantitative analysis of complex drug-drug interactions between cerivastatin and metabolism/transport inhibitors using physiologically based pharmacokinetic modeling*, *Drug Metabolism and Disposition*, 46 (2018), pp. 924–933.
- [19] K. YOSHIDA, K. MAEDA, H. KUSUHARA, AND A. KONAGAYA, *Estimation of feasible solution space using Cluster Newton Method: application to pharmacokinetic analysis of irinotecan with physiologically-based pharmacokinetic models.*, *BMC systems biology*, 7 Suppl 3 (2013), p. S3, <https://doi.org/10.1186/1752-0509-7-S3-S3>, <http://www.pubmedcentral.nih.gov/articlerender.fcgi?artid=3852065&tool=pmcentrez&rendertype=abstract>.
- [20] T. YOSHIKADO, K. YOSHIDA, N. KOTANI, T. NAKADA, R. ASAUMI, K. TOSHIMOTO, K. MAEDA, H. KUSUHARA, AND Y. SUGIYAMA, *Quantitative analyses of hepatic oatp-mediated interactions between statins and inhibitors using pbpk modeling with a parameter optimization method*, *Clinical Pharmacology & Therapeutics*, 100 (2016), pp. 513–523.
- [21] H. ZHANG, A. R. CONN, AND K. SCHEINBERG, *A derivative-free algorithm for least-squares minimization*, *SIAM Journal on Optimization*, 20 (2010), pp. 3555–3576.